DOI: http://dx.doi.org/10.12989/scs.2012.12.4.353

# Accuracy of combination rules and individual effect correlation: MDOF vs SDOF systems

Alfredo Reyes-Salazar*[1], Federico Valenzuela-Beltran[1], David de Leon-Escobedo[2], Eden Bojorquez[1] and Arturo López-Barraza[1]

[1]*Facultad de Ingeniería, Universidad Autónoma de Sinaloa, Ciudad Universitaria, Culiacán Sinaloa, México*
[2]*Facultad de Ingeniería, Universidad Autónoma del Estado de México, Ciudad Universitaria, Toluca, Estado de México, México*

*(Received September 07, 2011, Revised February 10, 2012, Accepted February 20, 2012)*

**Abstract.** The accuracy of the 30% and SRSS rules, commonly used to estimate the combined response of structures, and some related issues, are studied. For complex systems and earthquake loading, the principal components give the maximum seismic response. Both rules underestimate the axial load by about 10% and the COV of the underestimation is about 20%. Both rules overestimate the base shear by about 10%. The uncertainty in the estimation is much larger for axial load than for base shear, and, for axial load, it is much larger for inelastic than for elastic behavior. The effect of individual components may be highly correlated, not only for normal components, but also for totally uncorrelated components. The rules are not always inaccurate for large values of correlation coefficients of the individual effects, and small values of such coefficients are not always related to an accurate estimation of the response. Only for perfectly uncorrelated harmonic excitations and elastic analysis of SDOF systems, the individual effects of the components are uncorrelated and the rules accurately estimate the combined response. In the general case, the level of underestimation or overestimation depends on the degree of correlation of the components, the type of structural system, the response parameter, the location of the structural member and the level of structural deformation. The codes should be more specific regarding the application of these rules. If the percentage rule is used for MDOF systems and earthquake loading, at least a value of 45% should be used for the combination factor.

**Keywords:** seismic design codes; combination rules; effect of individual components; steel buildings; correlation of effects; MDOF and SDOF systems.

## 1. Introduction

After catastrophic damages during recent earthquakes around the world, seismic analysis and design procedures have been significantly modified. Several methods have been suggested in many codes including the equivalent lateral force procedure and several types of dynamic analysis procedures (modal response spectra analysis, linear time-history analysis, and nonlinear time-history analysis). Our understanding of the earthquake phenomenon has improved significantly during the last years. This improved understanding needs to be studied in the context of the estimation of structural responses since they are the primary interests of structural engineers. Due to the progress in the computer

* Corresponding author, Professor, E-mail: reyes@uas.uasnet.mx

technology, the computational capabilities have significantly increased in the recent years. It is now possible to estimate the seismic response behavior by modeling the structures in three dimensions and applying the seismic loadings in time domain as realistically as possible, satisfying the underlying physics. Responses obtained in this way may represent the best estimate and are considered to be the reference responses in this study. The accuracy of other simplified methods can then be judged by comparing the responses obtained by them to the reference responses. These comparisons are essential to improve our understandings and to design more seismic-load tolerant structures even by using simplified design procedures routinely used in the profession.

Energy released during an earthquake travels in the form of waves. They are measured in the form of two horizontal and one vertical translational acceleration time histories. Rotational excitations are not measured and are completely ignored in the analysis. In addition, for far-source ground motions, the effect of the vertical component is usually smaller than those of the horizontal components and is consequently neglected. Additional bases to neglect the vertical component effect are that building designs allow for gravity loads, which provides for a high factor of safety in the vertical direction (Newmark and Hall 1982, Salmon *et al.* 2009). Thus, when a structure is analyzed, two horizontal recorded components are generally applied along its horizontal structural principal axes. The orientation of the maximum response is sometimes ignored in the analysis.

In routine simplified analyses, structural responses are estimated by applying each component one at a time and then their effects are combined in many different ways. This concept has been implemented in many codes. The commonly used procedures are the 30 percent (30%) and the Square Root of Summation Squares (SRSS) combination rules. The requirements in International Building Code (IBC 2003) need to be satisfied at present in the U.S. Article 1620.2.10 of this code states "The direction of application of seismic forces used in design shall be that will produce the most critical load effect in each component. The requirement will be deemed satisfied if the design seismic forces are applied separately and independently in each of the two orthogonal directions." Later, in Article 1620.3.2 for the design of common structures with various plan irregularities belonging to Seismic Design Category C and D, IBC states "The critical direction requirement of Section 1620.2.10 will be deemed satisfied if one hundred percent of the forces in one direction are added to the 30 percent of the forces in the perpendicular direction. Alternatively, the effects of the two orthogonal directions are permitted to be combined on a square root of the sum of the squares (SRSS) basis. When the SRSS method of combining directional effects is used, each term computed shall be assigned the sign that will result in the most conservative result." The México City Code (RCDF 2004) states similar requirements for the evaluation of the combined responses of the seismic components. The codes, however, do not explicitly state the applicability of these rules. It is not specified how to select the critical orientation of the orthogonal components nor the type of structures (simple or complex systems) to be considered or if the rules can be applied to both, elastic and inelastic behavior. It is not specified either if the individual responses produced by each component should be collinear (axial load in columns) or non-collinear (base shear), or if the rules should be applied to single or simultaneously to multiple response parameters.

The rules implicitly assume that the components and their corresponding effects are uncorrelated. The accuracy of these combination rules, essentially developed for linear modal analysis procedures is studied in this paper. Some of the abovementioned issues are explicitly considered. The accuracy of the rules is estimated by comparing their results with the reference responses discussed earlier. The effect of the correlation of the components is considered. A computer program is developed by the authors for this purpose.

## 2. Literature review and objectives

The critical orientation of the earthquake components as well as the ways of combining their individual effects have been of interest to the civil engineering profession. Penzien and Watabe (1975) stated that the three components of an earthquake are uncorrelated along a set of axes generally denoted as principal axes. The major principal axis is horizontal and directed toward the epicenter, the intermediate axis is horizontal and perpendicular to the orientation of the major component, and the minor principal axis is vertical. The critical response could be obtained when these principal components are applied. Rosenblueth (1980) stated "lack of correlation of the principal accelerograms insures that responses are also uncorrelated". Smeby and Der Kiureghian (1985) observed that, for response spectra analysis of linear structures, when the two horizontal principal components are not along the structural principal axes, the effect of correlation is small and that if the two horizontal components have identical or nearly identical intensities, then the effect of correlation disappears. Newmark (1975) and Rosenblueth and Contreras (1977) proposed the *Percentage Rule* to approximate the combined response as the sum of the 100% of the response resulting from one component and some percentage ($\lambda$) of the responses resulting from the other two components. To combine the two horizontal components, Newmark (1975) suggested $\lambda$ to be 40% and Rosenblueth and Contreras (1977) suggested $\lambda$ to be 30%.

Many other studies were reported to combine the seismic responses due to two or three components. Using elastic analysis and a simple three-dimensional structure, Wilson *et al.* (1995) observed that the percent combination rule could underestimate the design forces in some members. Lopez *et al.* (2000) proposed a formula to calculate the critical value of structural responses due to the principal horizontal components acting along any incident angle with respect to the structural axes. Menun and Der Kiureghian (2000) developed a response-spectra-based procedure to predict the envelope that bounds the simultaneous action of two or more seismic response parameters for linear structures. For modal analysis, Der Kiureghian (1981) and Wilson *et al.* (1981) proposed the Complete Quadratic Combination (CQC) rule to combine modal responses due to a single seismic component. Smeby and Der Kiureghan (1985), Lopez and Torres (1996) and Lopez *et al.* (2004) proposed an extension of the CQC rule, known as the CQC3 rule, to combine modal responses due to two and three seismic components. They verified the CQC*3* rule by considering building-type structures with rectangular geometry and applied the rule to determine the critical response of elastic structures subjected to two and three seismic components with arbitrary spectra. Menun and Der Kiureghian (1998) extended these studies by considering more complex three-dimensional curved bridge structures subjected to two horizontal components. They compared the results of the CQC*3* rule with those of the SRSS, the 30% ($\lambda = 0.3$), and the 40% ($\lambda = 0.4$) rules. They concluded that the CQC3 rule is more appropriate because it accounts for the correlation of the components and because it is computationally simple. López *et al.* (2001) conducted a similar study to combine the two horizontal components with a range of one-story systems with symmetrical and unsymmetrical plan, and two multi-story buildings. Hernández and López (2003) extended the work of López *et al.* (2001) by considering the effect of the vertical component. The critical response was calculated for two cases: (i) assuming that a principal seismic component is along the vertical direction (CQC3 rule) and (ii) when a component does not coincide with the vertical direction (GCQC3 rule). They observed that if a principal component does not coincide with the vertical direction, the critical response would be underestimated using the GCQC3 rule. Lopez *et al.* (2006) investigated the response spectra characteristics of the principal components and determined the ratios between the spectra of the components. Beyer and Bommer (2007) studied several aspects involved when selecting and scaling records for bi-directional analysis post-processing the results of such analysis. They showed that the structural response varies depending on the angle of incidence of the ground motions with respect to the structural axes and that the median response for all possible angles could be the most appropriate quantity. Rigato and Medina (2007) examined the effect that the angle of incidence has on single-storey structure subjected to bi-directional ground motions. They demonstrated that applying bi-directional components along the principal axes of the structure could underestimate the inelastic peak demands. Nielson and DesRoches (2006), by using a three-dimensional analytical model, simulated the nonlinear seismic response of a typical multi-span simply supported steel girder bridge. They showed that, although the longitudinal loading of the bridge resulted in much larger demands compared with the transverse loading, some components of the bridge may still have appreciable damage under the transverse loading. They studies also indicated that modeling parameters such as loading direction and damping ratio are the most important in determining seismic response.

More recently, Kunnath *et al.* (2009) studied the seismic nonlinear response responses of typical highway overcrossings bridges subjected to combined effects of vertical and horizontal components for near-fault ground motions. They concluded that seismic demand analysis of ordinary highway bridges in general and overcrossings in particular should incorporate provisions to consider the effect of vertical component for near-fault ground motions. McKenna and Feneves (2009) investigated the effects of seismic force direction on the responses of slab-girder skewed bridges in response spectrum and time history linear dynamic analyses. The combination rules for orthogonal earthquake effects, such as the 100/30, 100/40percentage rules and the SRSS method were also examined. It was concluded that either the SRSS or the 100/40percentage rules could be used in the response spectrum analysis of skewed bridges. For time history analysis, however, none of the rules provide conservative results. The application of paired acceleration time histories in several angular directions is recommended. Lagaros (2010) implemented a multi-component incremental dynamic analysis procedure for three-dimensional structures. They used two components of seismic excitations for a sample of record-incident angle pairs. Bisadi and Head (2010) investigated the orthogonal effects in nonlinear analysis of single-span bridges subjected to multi-component earthquake excitations. They showed that the critical excitation angle is not the same in linear and nonlinear models and that the AASTHO procedure to estimate the combined effects of separate unidirectional excitations may underestimate the maximum probable response. Mackie and Cronin (2011) studied the effect of the incidence angle for three-dimensional excitation in the response of highway bridges. They computed single-degree-of-freedom elastic and inelastic mean spectra by using various orientation techniques. They found that the incidence angle has a negligible effect on mean ensemble response.

In spite of the important contributions of the previous studies on combination rules, most of them were limited to elastic analysis applied to structures modeled as SDOF systems or simplified plane concrete frames with a few stories connected by rigid diaphragms. They did not consider the inelastic behavior of the structural elements existing in actual structural systems and the appropriate energy dissipation mechanisms. Reyes-Salazar *et al.* (2000), Reyes-Salazar and Haldar (1999, 2000, 2001a, 2001b) and Bojorquez *et al.* (2010) found that strong-column weak-beam moment resisting steel frames are very efficient in dissipating earthquake-induced energy and that the dissipated energy has an important effect on the structural response. More recently, Reyes-Salazar *et al.* (2004, 2008), by using nonlinear time history analysis of complex multi-degree of freedom (MDOF) systems, observed that both the 30% and the SRSS rules could underestimate the combined response and that the energy dissipation mechanisms should be considered as accurately as possible. However, these studies did not consider realistic structural systems and did not estimate the effect of correlation of the earthquake components on the accuracy of the rules. The combination rules are re-examined considering more realistic and complex structural systems, the effect of correlation of the components, and the dissipation of energy in the structure. A more advanced nonlinear response analysis technique is used by considering the responses given by a computer program specifically developed for this purpose.

The above discussions clearly identify several issues that need our attention. The specific issues addressed in this study are: a) the critical orientation of the orthogonal components for collinear and non-collinear response quantities, b) the accuracy of the commonly used combination rules for complex MDOF systems for elastic and inelastic behavior and for collinear en non-collinear response parameters and c) the accuracy of the rules for SDOF systems. To comprehensively study these issues, the seismic responses of some structural models are estimated as accurately as possible by using a sophisticated three-dimensional time history analysis. The degree of correlation of the seismic components and their effects for the normally recorded and uncorrelated principal components are considered. The responses of steel buildings with moment resisting steel frames (MRSFs) are specifically studied.

## 3. Methodology and analysis procedure.

### *3.1 Methodology*

To satisfy the objectives of the study, the seismic responses of some steel building models are evaluated as accurately as possible using an efficient assumed stress-based finite element algorithm developed by the authors and their associates (Gao and Haldar 1995, Reyes-Salazar 1997). The procedure estimates nonlinear seismic responses in time domain considering material and geometry nonlinearities. In this approach, an explicit form of the tangent stiffness matrix is derived without any numerical integration. Fewer elements can be used in describing a large deformation configuration without sacrificing any accuracy, and the material and geometric nonlinearities can be incorporated without losing its basic simplicity. It gives very accurate results and is very efficient compared to the commonly used displacement-based approaches. The procedure and the algorithm, implemented in a computer program, have been extensively verified using available theoretical and experimental results (Reyes and Haldar 2000, Reyes and Haldar 2001b). The development of the theory of this approach is out of the scope of this study.

### *3.2 Structural models*

#### *3.2.1 Complex MDOF systems*

As part of the SAC steel project (FEMA 2000) three consulting firms were commissioned to perform the design of several model buildings. They were 3-, 9- and 20- story buildings which were designed according to the code requirements for the following three cities: Los Angeles (UBC 1994), Seattle (UBC 1994) and Boston (BOCA 1993). The 3- and 9- story buildings, representing Los Angeles area and the Pre-Northridge Designs, are considered in this study to address all the issues raised earlier. They will be denoted hereafter as Models 1 and 2, respectively. The elevations, plans models showing the location of moment resisting frames (continuous lines), and the particular elements considered in the study, are showed in Fig. 1. The beam and columns sections of the models are given in Table 1. The columns of the perimeter moment resisting frames (MRFs) of Model 1 are considered to be fixed at the

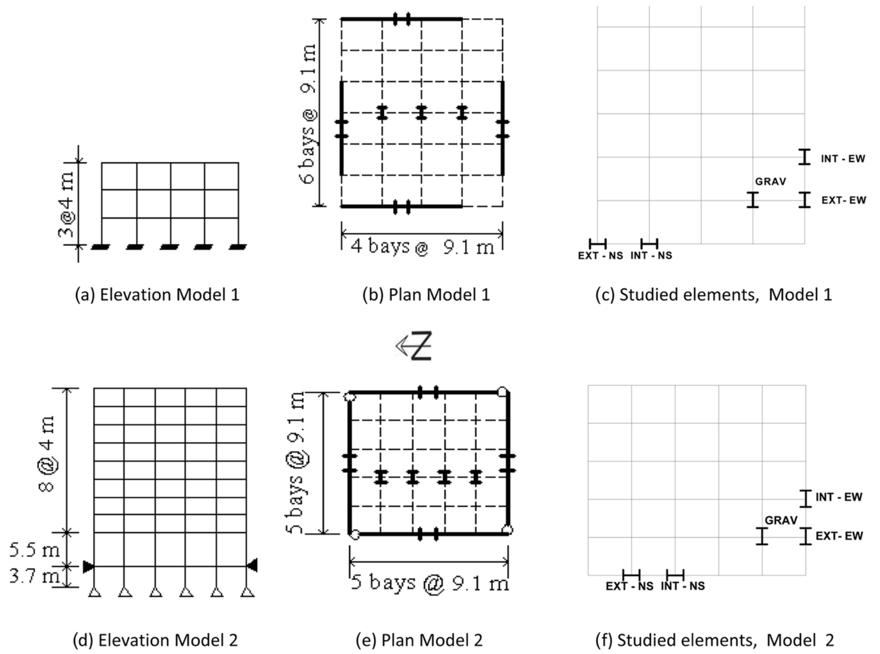


Fig. 1 Elevation, plan and element location for Models 1 and 2

Table 1 Beam and columns sections for Models 1 and 2

| Model | Story | Moment resisting frames | | | Gravity frames | | |
|---|---|---|---|---|---|---|---|
| | | Columns | | Girders | Columns | | Beams |
| | | Exterior | Interior | | Below penthouse | Others | |
| 1 | 1\2 | W14 × 257 | W14 × 311 | W33 × 118 | W14 × 82 | W14 × 68 | W18 × 35 |
| | 2\3 | W14 × 257 | W14 × 312 | W30 × 116 | W14 × 82 | W14 × 68 | W18 × 35 |
| | 3\Roof | W14 × 257 | W14 × 313 | W24 × 68 | W14 × 82 | W14 × 68 | W16 × 26 |
| 2 | -1/1 | W14 × 370 | W14 × 500 | W36 × 160 | W14 × 211 | W14 × 193 | W18 × 44 |
| | 1/2 | W14 × 370 | W14 × 500 | W36 × 160 | W14 × 211 | W14 × 193 | W18 × 35 |
| | 2/3 | W14 × 370 | W14 × 500, W14 × 455 | W36 × 160 | W14 × 211, W14 × 159 | W14 × 193, W14 × 145 | W18 × 35 |
| | 3/4 | W14 × 370 | W14 × 455 | W36 × 135 | W14 × 159 | W14 × 145 | W18 × 35 |
| | 4/5 | W14 × 370, W14 × 283 | W14 × 455, W14 × 370 | W36 × 135 | W14 × 159, W14 × 120 | W14 × 145, W14 × 109 | W18 × 35 |
| | 5/6 | W14 × 283 | W14 × 370 | W36 × 135 | W14 × 120 | W14 × 109 | W18 × 35 |
| | 6/7 | W14 × 283, W14 × 257 | W14 × 370, W14 × 283 | W36 × 135 | W14 × 120, W14 × 90 | W14 × 109, W14 × 82 | W18 × 35 |
| | 7/8 | W14 × 257 | W14 × 283 | W30 × 99 | W14 × 90 | W14 × 82 | W18 × 35 |
| | 8/9 | W14 × 257, W14 × 233 | W14 × 283, W14 × 257 | W27 × 84 | W14 × 90, W14 × 61 | W14 × 82, W14 × 48 | W18 × 35 |
| | 9/Roof | W14 × 233 | W14 × 257 | W24 × 68 | W14 × 61 | W14 × 48 | W16 × 26 |

base while those of Model 2 are assumed to be pinned. In all these frames, the columns are assumed to be made of Grade-50 steel and the girders are of A36 steel. For both models, the gravity columns are considered to be pinned at the base. Near rigid struts were used to consider the slab effect. All the columns in the perimeter MRFs bend about the strong axis. The strong axis of the gravity columns is oriented in the *N-S* direction. The designs of the MRFs in the two orthogonal directions were practically the same. The damping in the models is considered to be 5% of the critical damping; the same damping is used in the codified approaches. Steel structures were selected to study the addressed issues, but concrete structures could have been used. However, the authors thought it would be more interesting to work with steel structures because energy dissipation has a greater effect on the seismic response of these structures than on concrete structures. Moreover, the used models were suggested by FEMA (2000) and have been used for many researchers to study the seismic behavior of steel buildings with perimeter moment resisting steel frames and they can be considered as the benchmarks models. Additional information for the models can be obtained from the SAC steel project reports (FEMA 2000).

In seismic three-dimensional analysis of buildings, three degrees of freedoms are usually considered per floor; one rotational and two translational displacements. In this study, the frames are modeled as complex MDOF systems, i.e., each column is represented by one element and each girder of the perimeter MRFs is represented by two elements, having a node at the mid-span and considering six degrees of freedom per node. The total number of degrees of freedom is 846 and 3408, for Models 1 and 2, respectively. The models are excited by twenty recorded earthquake motions in time domain, recorded at different stations. They are presented in Table 2.

Table 2 Earthquake models

| No | Place | Year | Station | T (seg.) | ED (Km) | M | PGA (mm/s) |
|---|---|---|---|---|---|---|---|
| 1 | 1317 Mich. México | 1985 | Paraíso | 0.11 | 300 | 8.1 | 800 |
| 2 | 1634 Mammoth Lakes. USA | 1980 | Mammoth H. S. Gym | 0.12 | 19 | 6.5 | 2000 |
| 3 | 1634 Mammoth Lakes USA | 1980 | Convict Creek | 0.19 | 18 | 6.5 | 3000 |
| 4 | 1317 Mich. México | 1985 | Infiernillo N-120 | 0.21 | 67 | 8.1 | 3000 |
| 5 | 1317 Mich. México | 1985 | La Unión | 0.32 | 121 | 8.1 | 1656 |
| 6 | 1733 El Salvador | 2001 | Relaciones Ext. | 0.34 | 96 | 7.8 | 2500 |
| 7 | 1733 El Salvador | 2001 | Relaciones Ext. | 0.41 | 95 | 7.8 | 1500 |
| 8 | 1634 Mammoth Lakes. | 1980 | Long Valley Dam | 0.42 | 13 | 6.5 | 2000 |
| 9 | 2212 Delani Fault, AK | 2000 | K2-02 | 0.45 | 281 | 7.9 | 115 |
| 10 | 0836 Yountville CA | 2000 | Redwood City | 0.46 | 95 | 5.2 | 90 |
| 11 | 0408 Dillon MT | 2005 | MT:Kalispell | 0.51 | 338 | 5.6 | 51 |
| 12 | 1317 Mich. Mexico | 1985 | Villita | 0.53 | 80 | 8.1 | 1225 |
| 13 | 1232 Northrige | 1994 | Hall Valley | 0.54 | 25 | 6.4 | 2500 |
| 14 | 2115 Morgan Hill | 1984 | Hall Valley | 0.61 | 14 | 6.2 | 2000 |
| 15 | 2212 Delani Fault AK | 2002 | K2-04 | 0.62 | 290 | 7.9 | 133 |
| 16 | 0836 Yountville CA | 2000 | Dauville F.S. Ca | 0.63 | 73 | 5.2 | 144 |
| 17 | 0836 Yountville CA | 2000 | Pleasan Hill F.S. 1 | 0.71 | 92 | 5.2 | 74 |
| 18 | 0836 Yountville CA | 2000 | Pleasan Hill F.S. 2 | 0.75 | 58 | 5.2 | 201 |
| 19 | 2212 Delani Fault, AK | 2002 | Valdez City Hall | 0.85 | 272 | 7.9 | 260 |
| 20 | 1715 Park Fiel | 2004 | CA: Hollister City Hall | 1.01 | 147 | 6 | 145 |

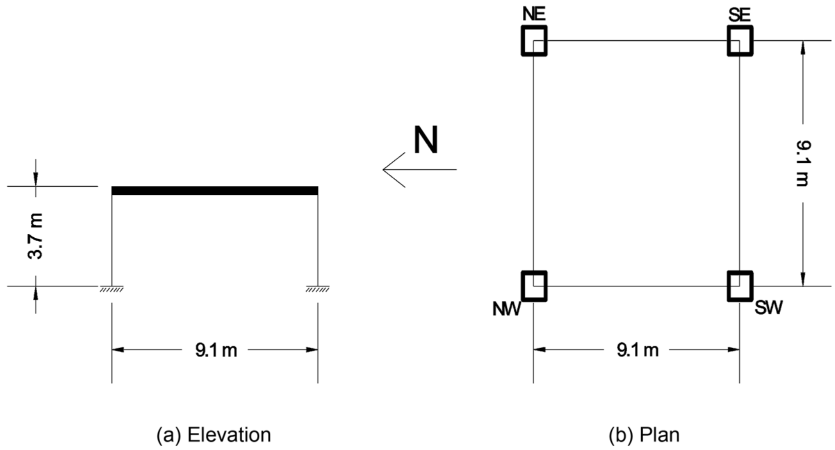


Fig. 2 Elevation and plan of the equivalent SDOF models (Models 1E and 2E)

### *3.2.2 SDOF systems*

The accuracy of the rules is also studied for equivalent SDOF systems. One equivalent SDOF model is considered for each MDOF system. These systems have a SDOF in each horizontal direction. They will be denoted hereafter as Model 1E and Model 2E. The elevation and plan of these systems are shown in Fig. 2. The weight of an equivalent SDOF system is the same as the total weight of its corresponding MDOF system and its lateral stiffness is selected in such a way that its natural period is the same as the fundamental natural period of its corresponding MDOF system. The damping ratio and the plastic moment are selected to be the same for both structural representations. It must be noted that in a strict sense, the simpler models are not the typical SDOF systems studied in the structural dynamics textbooks since axial forces can be developed in the columns under the action of horizontal excitations.

## *3.3 Combination rules*

The combination rules are formally defined in this part of the paper. The combination of the effects of the two horizontal components is specifically addressed. Collinear (axial load) and non-collinear (base shear) response parameters are considered. For the ease of discussion, $R_X$ will represent hereafter the maximum absolute load effect at a particular location when the structure is excited by the horizontal $X$ component of a given earthquake. Similarly, $R_Y$ will denote the corresponding maximum absolute load effect when the structure is excited by the horizontal $Y$ component of the earthquake. The load effects produced by each component can be calculated using various methods including the equivalent lateral load procedure, modal analysis, and time history analysis. For the time history analysis, elastic and inelastic analysis methods can be used to evaluate the load effects. Using the *Percentage* rule, the combined effect considering the two components can be calculated as

$$R_{C1} = R_X + \lambda R_Y \text{ or } R_{C1} = \lambda R_X + R_Y \tag{1}$$

If $\lambda = 0.3$, it represents the 30% combination rule. According to the SRSS rule, the combined response is given by

$$R_{C2} = \sqrt{R_X^2 + R_Y^2} \tag{2}$$

The basic assumption of the SRSS rule is that there is no correlation between the horizontal components. Obviously, if there were no correlation and the intensities of the components were identical, the corresponding value for $\lambda$ in Eq. (1) would be 0.414. These rules appear to be simple. However, they need critical review with respect to the issues raised earlier. By assuming the responses to be either elastic or inelastic, the overall combined or reference response can be estimated by simultaneously applying the two horizontal normal and principal components. The accuracy of the combination rules then can be studied by comparing the results with the reference responses.

### 3.4 Load cases

In order to meet the objectives of the study, several seismic and harmonic load cases need to be considered. Recorded horizontal time histories will be denoted as normal components. When they are transformed to uncorrelated components following the procedure suggested by Penzien and Watabe (1975) and Clough and Penzien (1993) they will be denoted, as stated earlier, as principal components. For the ease of discussion, the following notations will be used in the remainder of the paper. Considering the two horizontal components of an earthquake, the first horizontal component will be denoted as $X$ and the second horizontal component as $Y$. The symbols $X_n$ and $Y_n$ will indicate that the structures are excited by the normal components, and $X_p$ and $Y_p$ will indicate that the principal components are used instead. Hence, the notation $(X_n, Y_n)$ indicates that the structure is excited by the *first* and *second* normal components applied simultaneously to the *N-S* and *E-W* directions of the structure, respectively. Similarly, the notation $(0, X_p)$ indicates that the structure is excited by only the first principal component acting along the *E-W* direction. The following particular load cases are considered:

Case 1, the structures are simultaneously excited by the two normal components; the first component is acting along the *N-S* structural direction and the second along the other horizontal principal structural direction (*E-W*). This case is denoted as $(X_n, Y_n)$.

Case 2, same as Case 1, but the components are interchanged $(Y_n, X_n)$.

Case 3, the total response according to the 30% and the SRSS combination rules considering the following two sub-cases: a) $(X_n, 0)$ and b) $(0, Y_n)$.

Case 4, the total response according to the 30% and the SRSS combination rules considering the following two sub-cases: a) $(Y_n, 0)$ and b) $(0, X_n)$.

Similarly, another four cases of analysis are considered when the principal components are applied. They are: Case 5 $(X_p, Y_p)$, Case 6 $(Y_p, X_p)$, Case 7a $(X_p, 0)$, Case 7b $(0, Y_p)$, Case 8a $(Y_p, 0)$, Case 8b $(0, X_p)$. Thus, for two structures, twenty earthquakes, eight cases, and considering the responses to be elastic and inelastic, a total of 640 analyses of complex MDOF structures under seismic loading were required. For any response parameter (axial loads or base shear), the reference response for normal components, denoted hereafter as $R_n$, is considered to be the maximum response of Cases 1 and 2. Similarly, the reference response for the principal components, $R_p$, is considered to be the maximum response of Cases 5 and 6.

For harmonic acceleration of the base, the applied first and second horizontal components are denoted as $P_X$ an $P_Y$. This loading is completely defined in Section 4.3 of the paper. The required analyses are:

Case 9, the structures are simultaneously excited by the two harmonic components; the first component is acting along the *N-S* structural direction and the second along the other horizontal principal structural direction (*E-W*). This case is denoted as ($P_X$, $P_Y$).

Case 10, same as Case 9, but the components are interchanged ($P_Y$, $P_X$).

Case 11, the total response according to the 30% and the SRSS combination rules considering the following two sub-cases: a) ($P_X$, *0*) and b) (0, $P_Y$).

Case 12, the total response according to the 30% and the, SRSS combination rules considering the following two sub-cases: a) ($P_Y$, *0*) and b) (0, $P_X$).

## 4. Results and discussion

### 4.1 Maximum response

#### 4.1.1 Axial load

To study the critical orientation, the maximum response ratio *R,* defined as $R_p / R_n$, is introduced. *R* values for the axial loads acting on some columns of the base (Figs. 1(c) and 1(f)) produced by the twenty actual earthquake time histories for Models 1 and 2 are presented in Figs. 3(a) and 3(b), respectively. The plots clearly indicate that, for a given model, *R* values vary significantly with the particular earthquake being considered and the locations of the elements. The range of variation is from 0.70 to 1.44 for Model 1, while the range is from 0.77 to 1.29 for Model 2. However, no trend or pattern is observed. The results are analyzed statistically. The mean and coefficient of variation (COV) of *R* for different cases are summarized in Columns 3 and 4 of Table 3. Results indicate that the mean values of *R* are larger than unity in most of the cases and that the associated uncertainty is too large in many cases.

To study the effect of inelastic behaviour on the *R* parameter, the actual time histories were scaled up so that yielding was produced in all the models. Based on the past experience and for the uniformity of comparison, all the actual time histories were scaled up to develop a maximum average interstory drift of about 1.8 % by the trial and error procedure, instead of tracking the total number of plastic hinges developed. It was observed that about eight to sixteen plastic hinges were formed in the models when

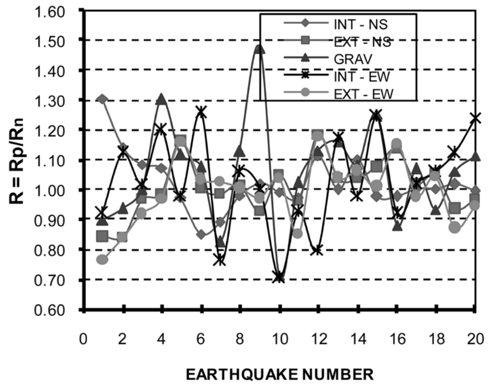


(a) Model 1

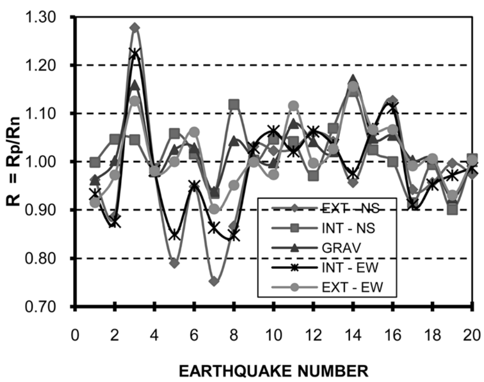


(b) Model 2

Fig. 3 Values of the *R* parameter for axial load and elastic behavior

Table 3 Statistics of the *R* ratio

| Model (1) | Element location (2) | | Elastic Mean (3) | Elastic COV (4) | Inelastic Mean (5) | Inelastic COV (6) |
|---|---|---|---|---|---|---|
| 1 | Axial load | INT-NS | 1.02 | 0.11 | 1.12 | 0.17 |
| | | EXT-NS | 1.01 | 0.09 | 1.01 | 0.05 |
| | | GRAV | 1.06 | 0.16 | 1.01 | 0.15 |
| | | INT-EW | 1.03 | 0.16 | 1.00 | 0.41 |
| | | EXT-EW | 0.99 | 0.11 | 1.03 | 0.05 |
| | | All elements | 1.02 | 0.13 | 1.07 | 0.21 |
| | Base shear | | 1.02 | 0.05 | 0.99 | 0.08 |
| 2 | Axial load | EXT-NS | 0.99 | 0.13 | 1.01 | 0.04 |
| | | INT-NS | 1.04 | 0.06 | 1.08 | 0.73 |
| | | GRAV | 1.02 | 0.06 | 0.99 | 0.08 |
| | | INT-EW | 0.98 | 0.12 | 1.00 | 0.05 |
| | | EXT-EW | 1.04 | 0.07 | 1.48 | 0.57 |
| | | All elements | 1.02 | 0.09 | 1.13 | 0.49 |
| | Base shear | | 1.01 | 0.03 | 1.02 | 0.06 |

they developed the desired drift. Plots similar to those previously discussed are then developed for both models, but they are not shown. It is observed that, the *R* values are significantly larger than unity in many of the cases. Their statistics are given in Columns 5 and 6 of Table 3. The results indicate that the principal components produce larger axial forces by about 7% and 13% for Model 1 and 2, respectively. The most important observation that can be made is that the mean value and COV significantly increase for some cases while changing from elastic to inelastic behavior. The increment in COV is larger than that of the mean.

### 4.1.2 Base shear

As for the case of axial load discussed earlier, $R$, $R_p$, and $R_n$ parameters are evaluated for base shear. Considering Case 1, the base shear in the $X$ direction produced by the simultaneous application of the two horizontal components is denoted as $V_x$. Similarly, the base shear in $Y$ direction produced by the simultaneous application of both components is denoted as $V_y$. Then, the *total base shear* $V_R$, is calculated as $V_R = \sqrt{V_x^2 + V_y^2}$. Similarly for Case *2*, another value for $V_R$ can be estimated. The larger of the two is considered to be, the reference value ($R_n$) for base shear for normal components. Following the same procedure and considering Cases 5 and 6, the reference value for principal components is obtained ($R_p$). Then, by taking the ratio $R_p/R_n$, the $R$ parameter for base shear is estimated. Similar plots to those of Fig. 3 developed for axial loads were also developed for base shear for both models and type of behaviors, but are not shown here, only the statistics are reported. The results are presented in Table 3. Results indicate that, as for the case of axial loads, the principal components give the larger response, although on the average the difference is quite small between the two sets of components. In general the mean values of $R$ and the uncertainty in its estimation are smaller for base shear than for axial load.

In summary, the principal components may produce about 13% larger axial load for the inelastic case, but statistically there are no differences in the estimation of axial load for the elastic case when excited

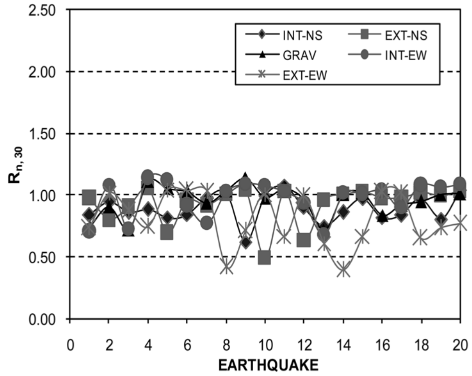


(a) $R_{n,\ 30}$ parameter, elastic behavior

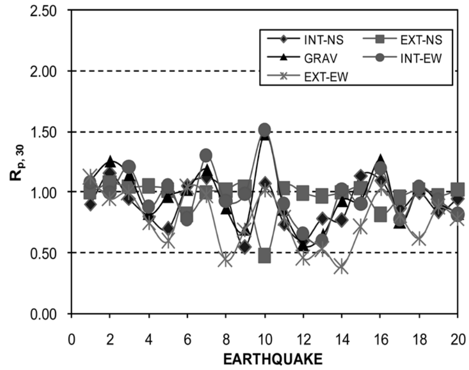


(b) $R_{p,\ 30}$ parameter, elastic behavior

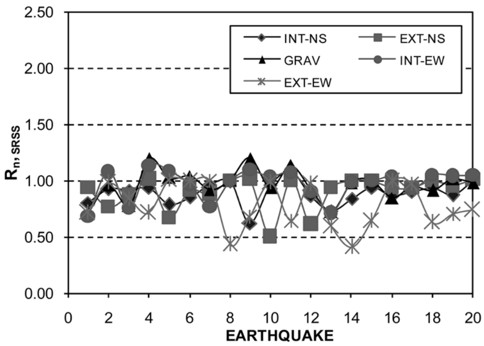


(c) $R_{n,\ SRSS}$ parameter, elastic behavior

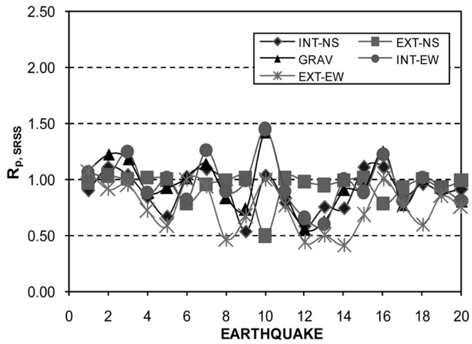


(d) $R_{p,\ SRSS}$ parameter, elastic behavior

Fig. 4 Accuracy of the 30% rule for MDOF systems and earthquake loading, Model 1

by normal or principal components. There may not be any major difference in estimating the base shear for both elastic and inelastic behaviors for normal and principal components. The uncertainty in the estimation is much larger for axial load than for base shear, particularly for inelastic behavior. Large COV in estimating the axial load for nonlinear structural behavior, could have some design implications.

### *4.2 Aplicability of the rules to MDOF systems*

#### *4.2.1 Accuracy of the 30% combination rule, axial load and elastic behavior*

Considering excitation given by Case 3 and the 30% combination rule, two possible combined responses can be calculated for normal components as: ${}^3X_n + 0.3\ {}^3Y_n$ and $0.3\ {}^3X_n + {}^3Y_n$, where ${}^3X_n$ and ${}^3Y_n$ are defined as the responses produced for Cases 3a and 3b, respectively. The larger of the two combined responses when normalized with respect to the *reference response* ($R_n$) defined earlier will give a random variable defined as ${}^3R_{n30}$. Following exactly the same procedure for Load Case 4, ${}^4R_{n30}$ can be calculated. The combination of both cases (${}^3R_{n,30}$, ${}^4R_{n,30}$) and 20 earthquakes give a total of 40 sample points. It will be denoted as the random variable $R_{n,30}$. Considering principal components and excitations given by load Cases 7 and 8, 40 sample points are similarly generated, it will be denoted as the random variable $R_{p,30}$. Typical values of $R_{n,30}$ and $R_{p,30}$ are presented in Figs. 4(a) and 4(b) for elastic

Table 4 Statistics for $R_{n,30}$, $R_{p,30}$, $R_{n,SRSS}$ and $R_{p,SRSS}$ for MDOF systems and earthquake loading, axial load and base shear, elastic behavior

| Model (1) | Column location (2) | | 30% Rule | | | | SRSS Rule | | | | Sample size (11) |
|---|---|---|---|---|---|---|---|---|---|---|---|
| | | | Normal $R_{n,30}$ | | Principal $R_{p,30}$ | | Normal $R_{n,SRSS}$ | | Principal $R_{p,SRSS}$ | | |
| | | | Mean (3) | COV (4) | Mean (5) | COV (6) | Mean (7) | COV (8) | Mean (9) | COV (10) | |
| 1 | Axial load | INT-NS | 0.90 | 0.12 | 0.92 | 0.21 | 0.89 | 0.11 | 0.91 | 0.19 | 40 |
| | | EXT-NS | 0.93 | 0.16 | 0.97 | 0.13 | 0.90 | 0.17 | 0.94 | 0.13 | 40 |
| | | GRAV | 0.96 | 0.13 | 0.97 | 0.24 | 0.96 | 0.14 | 0.96 | 0.23 | 40 |
| | | INT-EW | 0.98 | 0.14 | 0.98 | 0.22 | 0.97 | 0.14 | 0.97 | 0.22 | 40 |
| | | EXT-EW | 0.81 | 0.26 | 0.78 | 0.28 | 0.78 | 0.26 | 0.76 | 0.28 | 40 |
| | | All elements | 0.91 | 0.18 | 0.92 | 0.23 | 0.90 | 0.18 | 0.91 | 0.22 | 200 |
| | Base shear | | 1.07 | 0.07 | 1.07 | 0.09 | 1.09 | 0.07 | 1.09 | 0.09 | 40 |
| 2 | Axial load | EXT-NS | 0.91 | 0.22 | 0.92 | 0.16 | 0.88 | 0.22 | 0.90 | 0.17 | 40 |
| | | INT-NS | 0.95 | 0.09 | 0.99 | 0.12 | 0.94 | 0.11 | 0.97 | 0.12 | 40 |
| | | GRAV | 0.97 | 0.11 | 0.99 | 0.12 | 0.95 | 0.12 | 0.97 | 0.11 | 40 |
| | | INT-EW | 0.77 | 0.25 | 0.79 | 0.24 | 0.75 | 0.24 | 0.78 | 0.23 | 40 |
| | | EXT-EW | 0.95 | 0.14 | 0.99 | 0.13 | 0.94 | 0.14 | 0.97 | 0.12 | 40 |
| | | All elements | 0.91 | 0.19 | 0.94 | 0.17 | 0.89 | 0.18 | 0.92 | 0.17 | 200 |
| | Base shear | | 1.09 | 0.06 | 1.11 | 0.06 | 1.11 | 0.08 | 1.12 | 0.08 | 40 |

behavior and Model 1. It is observed that these parameters vary significantly with the particular earthquake being considered and the locations of the elements without showing any trend. For most of the cases the combined response is underestimated, values smaller than 50% are observed in many cases even for principal components. The statistics of $R_{n,30}$ and $R_{p,30}$ are summarized in Columns 3 through 6 of Table 4. The results clearly indicate that, on an average basis, the 30% combination rule underestimates the combined axial load by about 10% and that the uncertainty associated with the estimation is too large in some cases. The observations made for the normal components are essentially identical to that of principal components.

#### *4.2.2 Accuracy of the SRSS combination rule, axial load and elastic behavior*

Combined responses using the SRSS rule are then discussed. Normalized response parameter similar to those of the 30% rule are estimated. In this case the corresponding random variables are denoted as $R_{n,SRSS}$ and $R_{p,SRSS}$ for normal and principal components, respectively. The results for Model 1 are presented in Figs. 4(c) and 4(d) for elastic behavior. The major observations made for the 30% rule also apply to this rule. The corresponding statistics are summarized in columns 7 through 10 of Table 4. Results of the table indicate that, on an average basis, the SRSS rule underestimate the combined response. The statistics are essentially the same for both rules and for normal and principal components. It can be concluded that both, the 30% and the SRSS combination rules underestimate the axial load by about 10% for both, normal and principal components and that the uncertainty (COV) in the underestimation is about 20%. These results indicate that for complex MDOF systems, there is a certain degree of correlation between the effects of individual components of earthquakes, even for the case of uncorrelated components.

### 4.2.3 Accuracy of the 30% and SRSS combination rule, base shear, elastic behavior

The accuracy of the 30% and SRSS combination rules in the estimation of the total base shear is discussed next. The parameters ${}^3X_n$, ${}^3Y_n$, ${}^4X_n$, and ${}^4Y_n$ and so on are as defined earlier for axial load; the only difference is that now they represent base shear. The statistics of $R_{n,30}$, $R_{p,30}$, $R_{n,SRSS}$ and $R_{p,SRSS}$ for base shear are summarized in Table 4. The results indicate that, unlike the case of axial load, both rules reasonably overestimate the combined base shear. The overestimation is about 10% and is observed to be essentially the same for normal and principal components. The uncertainty in the estimation is much larger for axial load than for base shear.

### 4.2.4 Combination rules for inelastic behavior

The accuracy of the combination rules in the estimation of the combined axial load and base shear for inelastic structural behavior is now discussed. Similar plots to those of elastic behavior are also developed but are not shown. Only their statistics are reported, they are presented in Table 5. All the observation made for elastic behavior essentially remain the same for inelastic behavior. The only additional observation is that the uncertainty in the prediction significantly increases for axial load.

### 4.2.5 Correlation between individual effects.

The basic assumption of the SRSS rule is that there is no correlation between the horizontal components. It is implicitly assumed that if there is no correlation between the accelerograms, the corresponding effects will also be uncorrelated. The actual degree of correlation between the individual effects of the horizontal components and the effect of correlation on the accuracy of the rules are discussed in this section of the paper. The correlation coefficients (ρ) are estimated for Models 1 and 2,

Table 5 Statistics for $R_{n,30}$, $R_{p,30}$, $R_{n,SRSS}$ and $R_{p,SRSS}$ for MDOF systems and earthquake loading, axial load and base shear, inelastic behavior

| Model (1) | Column location (2) | | 30% Rule | | | | SRSS Rule | | | | Sample size (11) |
|---|---|---|---|---|---|---|---|---|---|---|---|
| | | | Normal $R_{n,30}$ | | Principal $R_{p,30}$ | | Normal $R_{n,SRSS}$ | | Principal $R_{p,SRSS}$ | | |
| | | | Mean (3) | COV (4) | Mean (5) | COV (6) | Mean (7) | COV (8) | Mean (9) | COV (10) | |
| 1 | Axial load | INT-NS | 0.84 | 0.43 | 0.90 | 0.43 | 0.83 | 0.43 | 0.88 | 0.44 | 40 |
| | | EXT-NS | 0.94 | 0.13 | 0.97 | 0.09 | 0.93 | 0.13 | 0.97 | 0.1 | 40 |
| | | GRAV | 0.99 | 0.23 | 1.01 | 0.22 | 1.00 | 0.22 | 1.01 | 0.22 | 40 |
| | | INT-EW | 0.84 | 0.61 | 0.8 | 0.64 | 0.81 | 0.62 | 0.78 | 0.64 | 40 |
| | | EXT-EW | 0.93 | 0.14 | 0.91 | 0.14 | 0.93 | 0.14 | 0.91 | 0.14 | 40 |
| | | All elements | 0.91 | 0.34 | 0.92 | 0.34 | 0.90 | 0.34 | 0.91 | 0.34 | 200 |
| | Base Shear | | 1.06 | 0.08 | 1.1 | 0.07 | 1.11 | 0.07 | 1.15 | 0.08 | 40 |
| 2 | Axial load | EXT-NS | 0.96 | 0.13 | 0.97 | 0.08 | 0.95 | 0.13 | 0.96 | 0.08 | 40 |
| | | INT-NS | 0.96 | 0.73 | 1.34 | 0.6 | 0.95 | 0.73 | 1.32 | 0.61 | 40 |
| | | GRAV | 1.03 | 0.16 | 1.1 | 0.15 | 1.03 | 0.15 | 1.08 | 0.16 | 40 |
| | | INT-EW | 0.83 | 0.23 | 0.84 | 0.2 | 0.82 | 0.23 | 0.83 | 0.2 | 40 |
| | | EXT-EW | 0.54 | 0.76 | 0.45 | 1.02 | 0.53 | 0.74 | 0.44 | 1.02 | 40 |
| | | All elements | 0.86 | 0.48 | 0.94 | 0.55 | 0.86 | 0.48 | 0.93 | 0.55 | 200 |
| | Base Shear | | 1.11 | 0.07 | 1.11 | 0.07 | 1.13 | 0.08 | 1.13 | 0.07 | 40 |

Table 6 Correlation coefficients (ρ) of the effect of individual components, MDOF systems and earthquake loading, axial load, Model 2

| Earth (1) | $\rho_{NO}$ (2) | Normal components | | | | | | Principal components | | | | | |
|---|---|---|---|---|---|---|---|---|---|---|---|---|---|
| | | Elastic | | | Inelastic | | | Elastic | | | Inelastic | | |
| | | EXT-NS (3) | INT-NS (4) | Shear (5) | EXT-NS (6) | INT-NS (7) | Shear (8) | EXT-NS (9) | INT-NS (10) | Shear (11) | EXT-NS (12) | INT-NS (13) | Shear (14) |
| 1 | 0.23 | -0.74 | 0.72 | 0.73 | -0.71 | -0.69 | 0.72 | 0.84 | 0.84 | 0.88 | 0.88 | 0.90 | 0.87 |
| 2 | -0.17 | -0.05 | 0.42 | 0.50 | -0.50 | -0.21 | 0.38 | 0.17 | 0.23 | 0.39 | 0.35 | 0.03 | 0.36 |
| 3 | 0.32 | 0.08 | 0.54 | 0.59 | -0.10 | -0.21 | 0.53 | -0.19 | 0.30 | 0.35 | -0.17 | 0.33 | 0.50 |
| 4 | -0.15 | 0.29 | 0.11 | 0.12 | 0.44 | 0.04 | 0.14 | 0.28 | 0.10 | 0.10 | 0.44 | 0.08 | 0.12 |
| 5 | -0.23 | -0.33 | 0.36 | 0.35 | -0.68 | -0.62 | 0.42 | 0.12 | -0.10 | -0.08 | -0.53 | -0.20 | -0.07 |
| 6 | 0.17 | 0.21 | 0.37 | 0.50 | 0.59 | 0.39 | 0.45 | 0.15 | 0.24 | 0.25 | -0.23 | 0.20 | 0.28 |
| 7 | 0.18 | 0.18 | 0.25 | 0.48 | 0.26 | 0.07 | 0.44 | -0.29 | 0.66 | 0.68 | -0.76 | -0.07 | 0.70 |
| 8 | 0.11 | -0.01 | 0.07 | 0.26 | -0.07 | 0.26 | 0.29 | -0.01 | -0.08 | -0.09 | 0.03 | 0.24 | -0.07 |
| 9 | 0.13 | 0.38 | -0.11 | -0.08 | 0.39 | 0.16 | -0.13 | 0.24 | -0.19 | -0.16 | 0.23 | 0.06 | -0.18 |
| 10 | 0.13 | 0.16 | 0.27 | 0.29 | -0.25 | 0.12 | 0.27 | 0.28 | 0.31 | 0.32 | -0.24 | 0.05 | 0.27 |
| 11 | -0.33 | 0.09 | 0.12 | 0.10 | 0.10 | 0.04 | 0.13 | -0.02 | -0.02 | 0.00 | 0.07 | -0.01 | -0.01 |
| 12 | -0.14 | -0.07 | 0.06 | 0.17 | 0.40 | 0.04 | 0.14 | -0.04 | -0.12 | -0.05 | -0.40 | 0.07 | 0.00 |
| 13 | 0.11 | 0.38 | 0.28 | 0.46 | 0.64 | 0.00 | 0.38 | 0.38 | 0.15 | 0.36 | 0.63 | -0.02 | 0.29 |
| 14 | 0.15 | -0.01 | 0.11 | 0.14 | -0.20 | -0.23 | 0.17 | -0.11 | 0.06 | 0.16 | -0.55 | -0.20 | 0.17 |
| 15 | 0.19 | 0.35 | 0.71 | 0.64 | 0.80 | 0.33 | 0.56 | 0.29 | 0.51 | 0.47 | 0.70 | 0.18 | 0.38 |
| 16 | 0.13 | 0.01 | -0.14 | -0.12 | 0.35 | -0.10 | -0.13 | -0.05 | -0.11 | -0.03 | 0.07 | -0.04 | -0.10 |
| 17 | -0.13 | -0.10 | 0.02 | 0.07 | 0.03 | 0.08 | 0.10 | -0.01 | 0.28 | 0.28 | -0.09 | -0.06 | 0.32 |
| 18 | -0.16 | 0.09 | 0.13 | 0.20 | 0.55 | 0.07 | 0.15 | 0.14 | 0.19 | 0.25 | 0.53 | -0.04 | 0.20 |
| 19 | 0.13 | -0.40 | 0.07 | 0.07 | -0.43 | -0.15 | 0.06 | -0.19 | -0.03 | -0.07 | -0.20 | -0.03 | -0.08 |
| 20 | 0.18 | -0.03 | -0.07 | -0.06 | -0.01 | 0.05 | 0.72 | -0.04 | -0.04 | -0.02 | -0.10 | 0.00 | 0.01 |

for normal and principal components, for elastic and inelastic behavior and for collinear (axial load) and non-collinear (base shear) response parameters. However, only a few results in terms of axial loads on some columns and total base shear of Model 2 are presented. The coefficients of correlation between the normal horizontal accelerograms ($\rho_{NO}$) are given in Column 2 of Table 6. It is observed that normally recorded components may be highly correlated. The corresponding coefficients for the principal accelerograms are obviously zero. The correlation coefficients of the individual effects are given in Columns (3) through (14). It is shown that the correlation values significantly vary from one earthquake to another and from one element to another. Most of the values can be considered negligible (smaller than 0.25). For many cases however, the correlation is significant. Values of $\rho$ larger than 0.5 are observed in many cases. From the results of Fig. 4 and Table 6, it is observed that the rules are not always inaccurate in the estimation of the combined response for large values of $\rho$. On the other hand, small values of the coefficients are not always related to an accurate estimation of combined response. The implication of this is that there may be other factors that influence the accuracy of the combination rules. It is discussed further in subsequent sections of the paper.

Based on the earlier results it can be concluded that, for MDOF systems and earthquake loading, both combination rules underestimate the axial load by about 10% and the COV of the underestimation is about 20%. Both rules overestimate the base shear by about 10% for normal and principal components.

The uncertainty in the estimation is much larger for axial load than for base shear. The mean axial loads and base shear values are essentially the same for elastic and inelastic behavior. However, the uncertainty in the prediction of axial load goes up significantly when inelastic behavior is considered. The effects of individual uncorrelated components (principal components) may be highly correlated. It is observed, for normal and principal components, that the rules are not always inaccurate in the estimation of the combined response for large values of correlation coefficients of the individual effects, and that small values of such coefficients are not always related to an accurate estimation of combined response. The implication of this is that there are other factors that should be considered while estimating the accuracy of the combination rules.

### 4.3 Accuracy of the rules for simpler systems and loading conditions

Even though our primary interest is to study the accuracy of the combination rules for complex MDOF systems subjected to earthquake loading, it may be helpful to study the accuracy of the rules for simpler systems and dynamics excitations. It will allow to know the degree of correlation of the components in advance and to eliminate the influence of the higher modes of vibration and of several frequencies of the earthquakes. It may give additional insights regarding the accuracy of the rules for complex structural systems. Moreover, it will make possible to compare the level of accuracy of the rules for structural systems of different complexity. Initially, the *equivalent* SDOF systems defined earlier in Section 3.2, under the action of harmonic acceleration of the base, are considered. Then, the same SDOF systems are assumed to be acted upon earthquake excitations. Finally, MDOF systems and harmonic excitation are considered.

#### 4.3.1 SDOF systems and harmonic loading

The accuracy of the rules and the correlation coefficients of the effects of the horizontal components for the *equivalent* SDOF systems subjected to a harmonic acceleration of the base are discussed in this section of the paper. The base acceleration in the *N-S* structural direction is

$$P_X(t) = P_0 sin\,\omega t \tag{3}$$

and that of the *E-W* direction is given by

$$P_Y(t) = P_0 sin(\omega t + \phi) \tag{4}$$

where $P_0$ and $\omega$ are the amplitude and the frequency of the harmonic acceleration which are assumed to be 200 mm/sec$^2$ and 20 rad/sec, respectively. $\phi$ is the phase angle between the orthogonal horizontal accelerations which defines the degree of correlation of the harmonic components. $\phi$ = 0$^o$ and 90$^o$ correspond to totally correlated and uncorrelated components, respectively. As for the case of earthquake loading and MDOF systems, elastic and inelastic structural behaviors are considered. Thus, $P_X$ and $P_Y$ are first applied as defined above and then they are scaled up to produce significantly yielding in the models.

The responses of the equivalent systems are estimated, first, for each acceleration component applied separately (Load Cases 11 and 12) and then for the simultaneous action of both accelerations (Load cases 9 and 10). After that, the accuracies of the rules are calculated. The $R_{30}$ and $R_{SRSS}$ parameters are used for this purpose. They are essentially the same as $R_{n,30}$ and $R_{n,SRSS,}$ but now harmonic loading is

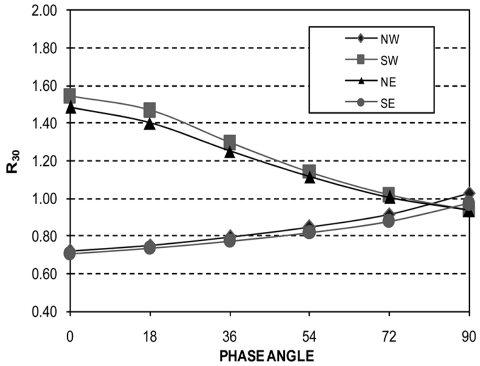


(a) $R_{30}$ parameter, elastic behavior

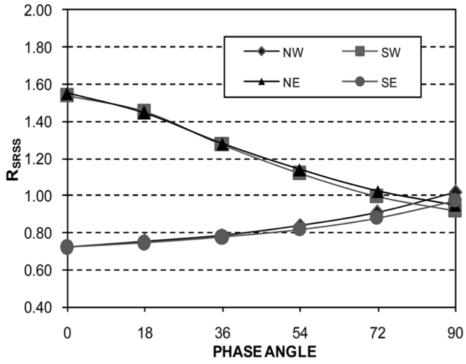


(b) $R_{SRSS}$ parameter, elastic behavior

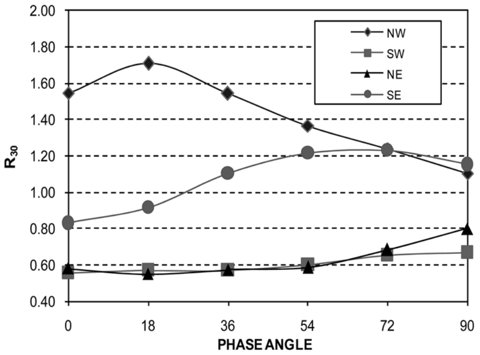


(c) $R_{30}$ parameter, inelastic behavior

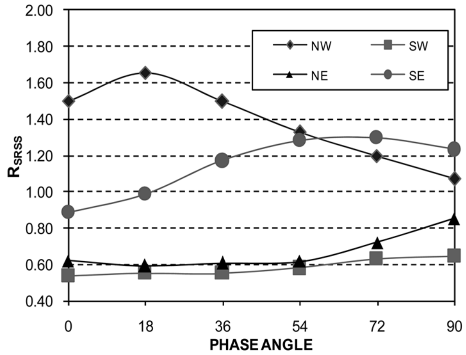


(d) $R_{SRSS}$ parameter, inelastic behavior

Fig. 5 Accuracy of the rules for SDOF systems and harmonic loading, Model 1E

used instead. The results for axial loads in the columns of Model 1E are presented in Figs. 5(a) and 5(b) for the 30% and SRSS rules, respectively, for elastic behavior. It must be noted that the values of $R_{30}$ and $R_{SRSS}$ are estimated for increments of $\phi$ of 18º. It is observed, in general, that if $\phi \leq 72º$, both rules may underestimate (columns NW and SE in Fig. 2) or overestimate (columns NE and SW) the combined response. The level of underestimation or overestimation monotonically increases as the values of the phase angle decrease (increasing correlation). However, the rules accurately estimate the combined axial load for all the columns when the phase angle is 90º, it is when the horizontal accelerations are totally uncorrelated. The results for inelastic behavior are shown in Figs. 5(c) and 5(d). Unlike the case of elastic behavior, the values of $R_{30}$ and $R_{SRSS}$ don´t monotonically tend to unity as $\phi$ varies from 0 to 90º. It indicates that the elastic response of structures subjected to dynamic loading may be quite different than that of the inelastic response. Even for uncorrelated components there is an important level of underestimation (up to 35%) or overestimation (up to 25%). Plots for base shear were also developed but are not shown. However, it is shown that for elastic behavior both rules reasonable overestimate the combined response for both rules and all values of $\phi$, the level of overestimation ranges from 5 to 15%. For the case of inelastic behavior the base shear is slightly underestimated (by about 5%) particularly for small values of $\phi$.

Plots for the $R_{30}$ and $R_{SRSS}$, parameters, for axial load and base shear, are also estimated for Model 2E

Table 7 Correlation coefficients (ρ) of the effect of individual components, harmonic loading, Model 1E, axial load

| Earth (1) | ρ (2) | Elastic | | | | Inelastic | | | |
|---|---|---|---|---|---|---|---|---|---|
| | | NW (3) | SW (4) | NE (5) | SE (6) | NW (7) | SW (8) | NE (9) | SE (10) |
| 1.00 | 0.97 | -0.97 | -0.97 | 0.97 | 1.00 | -0.74 | 0.74 | -0.86 | 0.86 |
| 0.95 | 0.91 | -0.91 | -0.91 | 0.91 | 0.95 | -0.74 | 0.74 | -0.85 | 0.85 |
| 0.81 | 0.77 | -0.77 | -0.77 | 0.77 | 0.81 | -0.66 | 0.66 | -0.76 | 0.76 |
| 0.59 | 0.55 | -0.55 | -0.55 | 0.55 | 0.59 | -0.53 | 0.53 | -0.59 | 0.59 |
| 0.31 | 0.27 | -0.27 | -0.27 | 0.27 | 0.31 | -0.33 | 0.33 | -0.36 | 0.36 |
| 0.00 | -0.03 | 0.03 | 0.03 | -0.03 | 0.00 | -0.10 | 0.10 | -0.11 | 0.11 |

but the results are not showed. The main observations made for Model 1E also apply to Model 2E. The only differences that can be mentioned is that the values of the underestimation or overestimation, for the case of axial load, are smaller for Model 2E, and that the base shear, unlike the case of Model 1E, is reasonably overestimated for all values of $\phi$, for elastic and inelastic behavior.

The correlation coefficients of the horizontal harmonic accelerations and those of their individual effects are given in Table 7 only for axial loads on columns of Model 1E, for elastic and inelastic behavior. As expected, for this simple loading and structural system, the correlations of the individual effects decrease as the correlation of the horizontal harmonic excitation decreases. The base shear follows a similar trend. The corresponding results for Model 2E were also estimated but are not given. The major conclusions, however, are the same than those of Model 1E.

From the results of Table 7 and Fig. 5 it is observed, in general, that totally correlated components don’t necessarily imply an underestimation of the combined response and that perfectly uncorrelated components don’t necessarily imply that the rules accurately will estimate the combined response. For example, for elastic behavior, whether the axial load is underestimated or not will depend, not only on the degree of correlation of the components, but also on the location of the column. For highly correlated components, say $\phi = 0^{o}$, the rules underestimate the combined axial load for *NW* and *SE* columns while they overestimate the response for *SW* and *NE* columns. The reason for this is that in the calculation of the reference axial load (axial load due to the simultaneous action of both components) the contribution of each component are in phase each other for the *NW* and *SE* columns but they are out phase for the others. Thus, large reference responses are obtained for the *NW* and *SE* columns and consequently an underestimation of the combined response. Moreover, as discussed before, for inelastic behavior, the values of the $R_{30}$ and $R_{SRSS}$ parameters vary from one column location to another and from one angle phase to another without showing any trend. It clearly indicates that the level of structural deformation is an important factor that, in general, must be considered while estimated the combined response according to the rules. It can be said that inelastic behavior introduces some *kind of correlation*. These results for SDOF systems and harmonic excitation clearly illustrate that there are several parameters that influence the accuracy of the rules. These parameters are also present in the case of MDOF systems and earthquake loading. Obviously in this case there are other factors that may have an important effect on the accuracy of the rules, as the frequency contents of the earthquakes, higher mode of vibrations of the systems and mass and stiffness distribution, which are not explicitly addressed in this study.

In summary, for elastic SDOF systems and harmonic loading, the 30% and SRSS rules may underestimate or overestimate the combined axial load for correlated components. For uncorrelated

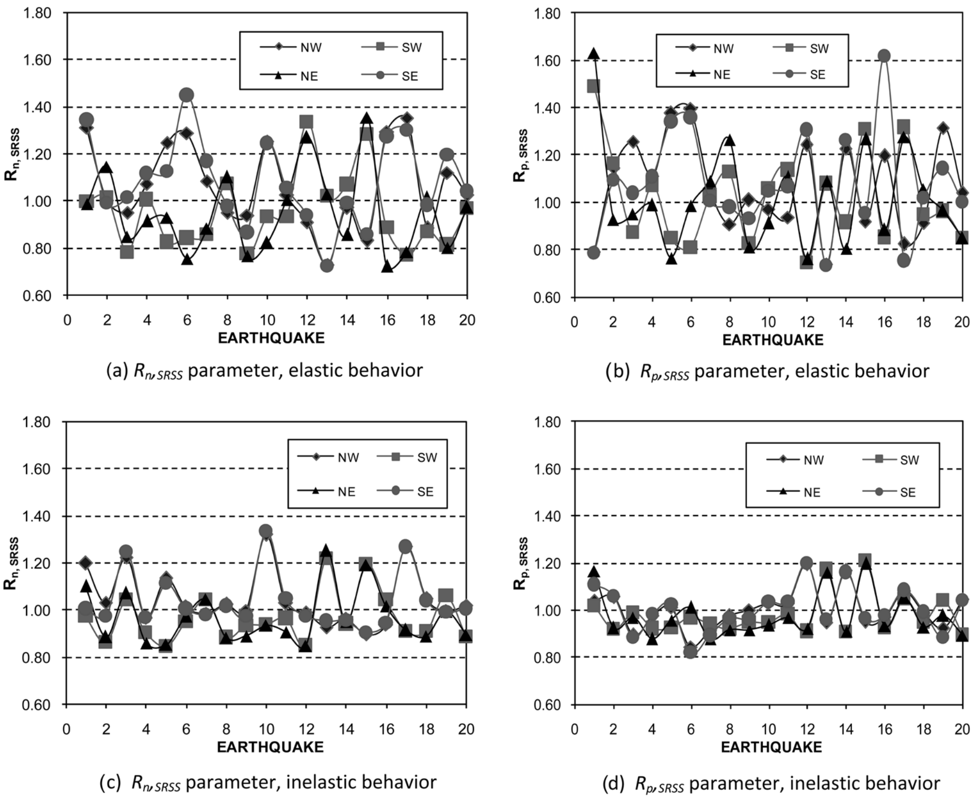


Fig. 6 Accuracy of SRSS rule for SDOF systems and earthquake loading, Model 1E

components, the rules accurately estimate the elastic axial load. However, for inelastic behavior, the rules may underestimate or overestimate the combined axial load even for uncorrelated components. The combined base shear is reasonably overestimated practically in all the cases. Thus, the level of underestimation or overestimation of the rules vary with the level of correlation of the components, the type of response parameter, the location of the structural member under consideration and the level of structural deformation.

### *4.3.2 SDOF systems and earthquake loading*

As for MDOF systems and earthquake loading, the $R_{p,30}$, $R_{p\ SRSS}$, $R_{n,30}$ and $R_{n\ SRSS}$ parameters will be used to represent the accuracy of the rules. The results for the SRSS rule and axial loads on columns of Model 1E are given in Fig. 6 for elastic and inelastic behavior. As for the MDOF systems and earthquake loading case, the values of $R_{n,SRSS}$ and $R_{p,SRSS}$ vary for one earthquake to another and from one column to another without showing any trend. However, unlike the case of MDOF systems both of the rules seem on an average basis to accurately estimate the combined response. Similar plots are also developed for the 30% rules but results are not presented, the major observations made for the SRSS rules apply to the 30% rule. Results in terms of base shear are also estimated but are not shown either. As for the case of MDOF systems, both rules reasonable overestimate the combined base shear, the only additional observation that can be made is that the level of overestimation is slightly larger for

Table 8 Statistics for $R_{n,30}$, $R_{p,30}$, $R_{n,SRSS}$ and $R_{p,SRSS}$ for SDOF systems and earthquake loading, axial load and base shear, elastic behavior

| Model (1) | Column location (2) | | *30%* Rule | | | | *SRSS* Rule | | | | Sample size (11) |
|---|---|---|---|---|---|---|---|---|---|---|---|
| | | | Normal $R_{n,30}$ | | Principal $R_{P,30}$ | | Normal $R_{n,30}$ | | Principal $R_{P,30}$ | | |
| | | | Mean (3) | COV (4) | Mean (5) | COV (6) | Mean (7) | COV (8) | Mean (9) | COV (10) | |
| 1E | Axial load | NW | 1.05 | 0.17 | 1.06 | 0.20 | 1.06 | 0.18 | 1.07 | 0.19 | 40 |
| | | NS | 1.01 | 0.35 | 1.07 | 0.35 | 1.02 | 0.36 | 1.08 | 0.35 | 40 |
| | | NE | 1.01 | 0.40 | 1.08 | 0.39 | 1.03 | 0.40 | 1.09 | 0.40 | 40 |
| | | SE | 1.06 | 0.17 | 1.07 | 0.23 | 1.08 | 0.18 | 1.08 | 0.22 | 40 |
| | | All columns | 1.03 | 0.29 | 1.07 | 0.30 | 1.05 | 0.29 | 1.08 | 0.30 | 160 |
| | Base shear | | 1.11 | 0.07 | 1.14 | 0.07 | 1.13 | 0.08 | 1.16 | 0.10 | 40 |
| 2E | Axial load | NW | 1.09 | 0.22 | 1.17 | 0.31 | 1.07 | 0.21 | 1.16 | 0.29 | 40 |
| | | NS | 1.06 | 0.23 | 1.10 | 0.37 | 1.06 | 0.24 | 1.10 | 0.37 | 40 |
| | | NE | 1.05 | 0.23 | 1.09 | 0.50 | 1.05 | 0.22 | 1.09 | 0.50 | 40 |
| | | SE | 1.08 | 0.25 | 1.14 | 0.31 | 1.09 | 0.25 | 1.14 | 0.30 | 40 |
| | | All columns | 1.07 | 0.23 | 1.12 | 0.37 | 1.07 | 0.23 | 1.13 | 0.37 | 160 |
| | Base shear | | 1.12 | 0.06 | 1.11 | 0.07 | 1.13 | 0.08 | 1.13 | 0.08 | 40 |

Table 9 Statistics for $R_{n,30}$, $R_{p,30}$, $R_{n,SRSS}$ and $R_{p,SRSS}$ for SDOF systems and earthquake loading, axial load and base shear, inelastic behavior

| Mmodel (1) | Column location (2) | | *30%* Rule | | | | *SRSS* Rule | | | | Sample size (11) |
|---|---|---|---|---|---|---|---|---|---|---|---|
| | | | Normal $R_{n,30}$ | | Principal $R_{P,30}$ | | Normal $R_{n,30}$ | | Principal $R_{P,30}$ | | |
| | | | Mean (3) | COV (4) | Mean (5) | COV (6) | Mean (7) | COV (8) | Mean (9) | COV (10) | |
| 1E | Axial load | NW | 1.09 | 0.12 | 1.04 | 0.09 | 1.05 | 0.12 | 1.00 | 0.09 | 40 |
| | | NS | 1.01 | 0.11 | 1.05 | 0.17 | 0.97 | 0.10 | 1.02 | 0.20 | 40 |
| | | NE | 1.00 | 0.12 | 1.01 | 0.10 | 0.97 | 0.11 | 0.98 | 0.10 | 40 |
| | | SE | 1.07 | 0.12 | 1.04 | 0.10 | 1.04 | 0.12 | 1.00 | 0.09 | 40 |
| | | All columns | 1.04 | 0.12 | 1.04 | 0.12 | 1.01 | 0.12 | 1.00 | 0.13 | 160 |
| | Base shear | | 1.09 | 0.05 | 1.09 | 0.05 | 1.05 | 0.05 | 1.05 | 0.04 | 40 |
| 2E | Axial load | NW | 1.04 | 0.21 | 1.11 | 0.40 | 1.03 | 0.20 | 1.13 | 0.41 | 40 |
| | | NS | 1.02 | 0.21 | 1.08 | 0.64 | 1.02 | 0.20 | 1.10 | 0.70 | 40 |
| | | NE | 1.01 | 0.21 | 1.08 | 0.64 | 1.01 | 0.20 | 1.11 | 0.71 | 40 |
| | | SE | 1.04 | 0.20 | 1.13 | 0.41 | 1.04 | 0.20 | 1.14 | 0.42 | 40 |
| | | All columns | 1.03 | 0.20 | 1.10 | 0.53 | 1.02 | 0.20 | 1.12 | 0.57 | 160 |
| | Base shear | | 1.12 | 0.07 | 1.10 | 0.08 | 1.12 | 0.08 | 1.12 | 0.09 | 40 |

SDOF systems. Model 2E is also studied but the results are not shown, the major conclusions are essentially the same than that of Model 1E. However, they are not shown, only their statistics are discussed.

The statistics of $R_{p,30}$, $R_{p\ SRSS}$, $R_{n,30}$, and $R_{n\ SRSS}$ for axial load and base shear are presented in Tables 8

Table 10 Correlation coefficients (ρ) of the effect of individual components, SDOF systems and earthquake loading, Model 2

| Earth (1) | $\rho_{NO}$ (2) | Normal components | | | | | | Principal components | | | | | |
|---|---|---|---|---|---|---|---|---|---|---|---|---|---|
| | | Elastic | | | Inelastic | | | Elastic | | | Inelastic | | |
| | | NW (3) | SW (4) | Shear (5) | NW (6) | SW (7) | Shear (8) | NW (9) | SW (10) | Shear (11) | NW (12) | SW (13) | Shear (14) |
| 1 | 0.23 | -0.70 | 0.70 | 0.71 | -0.71 | 0.71 | 0.72 | 0.90 | -0.90 | 0.90 | 0.85 | -0.85 | 0.84 |
| 2 | -0.17 | -0.11 | 0.10 | 0.31 | -0.01 | 0.01 | 0.28 | -0.06 | 0.09 | 0.33 | -0.04 | 0.04 | 0.33 |
| 3 | 0.32 | -0.30 | 0.33 | 0.38 | -0.17 | 0.17 | 0.39 | -0.69 | 0.72 | 0.51 | -0.70 | 0.70 | 0.49 |
| 4 | -0.15 | 0.50 | -0.53 | -0.12 | 0.50 | -0.50 | -0.10 | 0.38 | -0.42 | -0.34 | 0.37 | -0.37 | -0.35 |
| 5 | -0.23 | -0.76 | 0.76 | 0.44 | -0.76 | 0.76 | 0.44 | -0.65 | 0.65 | -0.06 | -0.57 | 0.57 | -0.11 |
| 6 | 0.17 | 0.59 | -0.59 | 0.61 | 0.57 | -0.57 | 0.58 | -0.19 | 0.16 | 0.25 | -0.05 | 0.05 | 0.21 |
| 7 | 0.18 | 0.35 | -0.36 | 0.43 | 0.36 | -0.36 | 0.43 | -0.79 | 0.81 | 0.74 | -0.77 | 0.77 | 0.69 |
| 8 | 0.11 | -0.20 | 0.20 | 0.41 | -0.22 | 0.22 | 0.42 | -0.05 | 0.04 | 0.00 | -0.02 | 0.01 | -0.01 |
| 9 | 0.13 | 0.25 | -0.26 | -0.11 | 0.26 | -0.26 | -0.10 | 0.09 | -0.10 | -0.07 | 0.10 | -0.10 | -0.05 |
| 10 | 0.13 | -0.49 | 0.51 | 0.44 | -0.45 | 0.45 | 0.47 | -0.57 | 0.58 | 0.59 | -0.60 | 0.59 | 0.63 |
| 11 | -0.33 | 0.09 | -0.09 | 0.10 | 0.11 | -0.11 | 0.08 | -0.08 | 0.08 | 0.09 | -0.04 | 0.04 | 0.08 |
| 12 | -0.14 | 0.35 | -0.33 | 0.29 | 0.40 | -0.40 | 0.31 | -0.54 | 0.50 | 0.33 | -0.51 | 0.51 | 0.33 |
| 13 | 0.11 | 0.11 | -0.15 | 0.19 | 0.17 | -0.17 | 0.20 | 0.11 | -0.14 | 0.22 | 0.13 | -0.13 | 0.21 |
| 14 | 0.15 | -0.53 | 0.55 | 0.33 | -0.59 | 0.60 | 0.37 | -0.70 | 0.72 | 0.43 | -0.74 | 0.74 | 0.42 |
| 15 | 0.19 | 0.55 | -0.56 | 0.25 | 0.56 | -0.56 | 0.25 | 0.43 | -0.44 | 0.10 | 0.43 | -0.43 | 0.09 |
| 16 | 0.13 | 0.10 | -0.16 | 0.25 | 0.16 | -0.15 | 0.26 | -0.23 | 0.22 | 0.18 | -0.02 | 0.02 | 0.19 |
| 17 | -0.13 | -0.09 | 0.11 | -0.15 | -0.01 | 0.01 | -0.18 | 0.10 | -0.12 | -0.02 | 0.07 | -0.07 | 0.05 |
| 18 | -0.16 | 0.77 | -0.75 | 0.01 | 0.76 | -0.75 | 0.00 | 0.76 | -0.73 | 0.11 | 0.75 | -0.75 | 0.10 |
| 19 | 0.13 | -0.51 | 0.50 | 0.16 | -0.42 | 0.42 | 0.10 | -0.46 | 0.46 | 0.01 | -0.37 | 0.37 | -0.04 |
| 20 | 0.18 | -0.13 | 0.15 | 0.14 | -0.17 | 0.17 | 0.15 | -0.14 | 0.16 | 0.09 | -0.17 | 0.17 | 0.10 |

and 9 for elastic and inelastic behavior, respectively. It is observed that, as stated earlier for individual plots, on an average basis, both rules reasonable overestimate the combined response for both, axial loads and base shear. The level of overestimation is, in general, larger for base shear than for axial load and the uncertainty in the estimation is much larger for axial load. For the case of axial load, the overestimation in terms of mean values is larger for principal than for normal components but it is quite similar for total base shear. The uncertainty in the estimation is similar for the 30% and the SRSS rules but can be quite different for normal and principal components.

The correlation coefficients (ρ) for both, axial load and total base shear are discussed next. Only the *NW* and *SW* columns and base shear of Model 2 are considered. The results are given in Table 10. Results indicate that, as for the case of MDOF systems, the ñ values are significant in many of the cases even for principal components. Thus, even for SDOF systems, if the horizontal accelerograms are uncorrelated it does not necessarily imply that their corresponding effects will also be uncorrelated.

From the results of this section of the paper it is concluded that, for the case of SDOF systems and earthquake loading, both rules reasonably overestimate the combined response in terms of axial load and total base shear, for elastic an inelastic behavior.

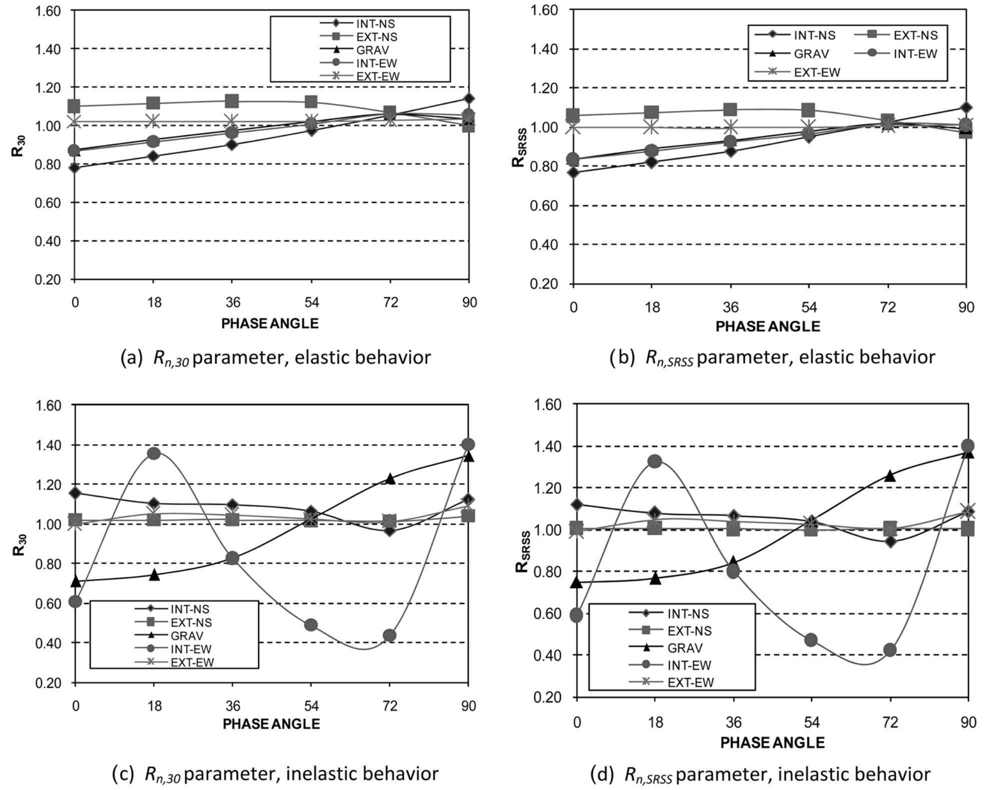


Fig. 7 Accuracy of the rules for MDOF systems and harmonic loading, Model 2

### *4.3.3 MDOF systems and harmonic loading*

The results for $R_{30}$ and $R_{SRSS}$ parameters for axial load and Model 2 are presented in Fig. 7. The major observations made before for SDOF systems and harmonic loading apply to this case: the 30% and SRSS rules may underestimate or overestimate the combined elastic axial load for highly correlated components. For totally uncorrelated components, the rules accurately estimate the elastic axial load. However, for inelastic behavior, the rules may underestimate or overestimate the combined axial load even for high values of the phase angle. The combined base shear is reasonably estimated practically in all the cases. The values of coefficients of correlation are also estimated but are not shown. They presented a similar trend as that of SDOF and harmonic loading.

From the results presented in this section and those presented in Section 4.2, it is concluded that only for the case of highly uncorrelated harmonic excitations and elastic analysis of SDOF systems, the individual effects of the components are uncorrelated and the 30% and SRSS rules accurately estimate the combined response. It is the authors' belief that the combination rules under consideration were developed for SDOF systems.

### *4.4 Combination factor*

The results presented in earlier sections showed that for MDOF systems and earthquake loading, the accuracy of the 30% rule in evaluating the combined response is essentially the same of the SRSS rule.

Table 11 Combinations factors ($\lambda_{req}$) for axial, Model 2 and earthquake loading, inelastic behavior

| Earth | EXT-NS | | | | INT-NS | | | | EXT-NS | | | | INT-NS | | | |
|---|---|---|---|---|---|---|---|---|---|---|---|---|---|---|---|---|
| | $^3R_n$ | $^4R_n$ | $^7R_P$ | $^8R_P$ | $^3R_n$ | $^4R_n$ | $^7R_P$ | $^8R_P$ | $^3R_n$ | $^4R_n$ | $^7R_P$ | $^8R_P$ | $^3R_n$ | $^4R_n$ | $^7R_P$ | $^8R_P$ |
| 1 | 0.29 | 0.62 | 0.89 | 0.98 | 0.89 | 0.93 | 0.67 | 0.78 | 0.90 | 0.11 | 0.69 | 0.88 | 0.41 | 0.84 | 0.66 | 0.78 |
| 2 | 0.58 | 0.03 | 0.54 | 0.39 | 0.26 | 0.29 | 0.15 | 0.21 | 0.24 | 0.88 | 0.53 | 0.31 | 0.73 | 0.22 | 0.19 | 0.76 |
| 3 | 0.43 | 0.59 | 0.33 | 0.67 | 0.82 | 0.72 | 0.43 | 0.27 | 0.55 | 0.55 | 0.68 | 0.53 | 0.65 | 0.96 | 0.92 | 0.64 |
| 4 | 0.29 | 0.43 | 0.46 | 0.60 | 0.24 | 0.17 | 0.41 | 0.32 | 0.46 | 0.14 | 0.85 | 0.29 | 0.17 | 0.57 | 0.34 | 0.78 |
| 5 | 0.40 | 0.97 | 0.13 | 0.78 | 0.30 | 0.67 | 0.00 | 0.23 | 0.98 | 0.25 | 0.80 | 0.00 | 0.44 | 0.99 | 0.22 | 0.71 |
| 6 | 0.98 | 0.50 | 0.23 | 0.15 | 0.78 | 0.59 | 0.16 | 0.16 | 0.28 | 0.58 | 0.50 | 0.11 | 0.56 | 0.50 | 0.08 | 0.99 |
| 7 | 0.37 | 0.45 | 0.85 | 0.94 | 0.21 | 0.64 | 0.71 | 0.77 | 0.98 | 0.17 | 0.93 | 0.52 | 0.22 | 0.66 | 0.57 | 0.22 |
| 8 | 0.26 | 0.82 | 0.44 | 0.28 | 0.43 | 0.41 | 0.08 | 0.22 | 0.49 | 0.36 | 0.79 | 0.03 | 0.43 | 0.38 | 0.04 | 0.21 |
| 9 | 0.36 | 0.54 | 0.19 | 0.27 | 0.18 | 0.42 | 0.03 | 0.40 | 0.87 | 0.49 | 0.89 | 0.23 | 0.04 | 0.69 | 0.00 | 0.63 |
| 10 | 0.32 | 0.55 | 0.65 | 0.37 | 0.40 | 0.29 | 0.63 | 0.58 | 0.33 | 0.33 | 0.30 | 0.76 | 0.38 | 0.91 | 0.62 | 0.82 |
| 11 | 0.45 | 0.20 | 0.26 | 0.24 | 0.45 | 0.50 | 0.15 | 0.29 | 0.39 | 0.23 | 0.18 | 0.52 | 0.33 | 0.25 | 0.12 | 0.45 |
| 12 | 0.43 | 0.95 | 0.32 | 0.25 | 0.38 | 0.34 | 0.05 | 0.15 | 0.79 | 0.45 | 0.01 | 0.49 | 0.21 | 0.32 | 0.10 | 0.02 |
| 13 | 0.16 | 0.39 | 0.14 | 0.51 | 0.14 | 0.46 | 0.29 | 0.61 | 0.31 | 0.13 | 0.38 | 0.22 | 0.25 | 0.25 | 0.15 | 0.36 |
| 14 | 0.55 | 0.58 | 0.20 | 0.09 | 0.26 | 0.47 | 0.33 | 0.29 | 0.47 | 0.65 | 0.99 | 0.17 | 0.24 | 0.77 | 0.12 | 0.91 |
| 15 | 0.54 | 0.70 | 0.37 | 0.72 | 0.69 | 0.60 | 0.53 | 0.57 | 0.62 | 0.30 | 0.20 | 0.16 | 0.67 | 0.22 | 0.55 | 0.61 |
| 16 | 0.24 | 0.66 | 0.08 | 0.23 | 0.38 | 0.20 | 0.18 | 0.12 | 0.62 | 0.18 | 1.06 | 0.13 | 0.13 | 0.63 | 0.33 | 0.72 |
| 17 | 0.19 | 0.79 | 0.28 | 0.11 | 0.39 | 0.28 | 0.63 | 0.55 | 0.86 | 0.33 | 0.34 | 0.08 | 0.27 | 0.33 | 0.69 | 0.75 |
| 18 | 0.29 | 0.90 | 0.27 | 0.79 | 0.32 | 0.45 | 0.33 | 0.31 | 0.81 | 0.24 | 0.69 | 0.17 | 0.30 | 0.29 | 0.16 | 0.22 |
| 19 | 0.57 | 0.14 | 0.78 | 0.18 | 0.24 | 0.18 | 0.12 | 0.20 | 0.09 | 0.36 | 0.09 | 0.51 | 0.40 | 0.07 | 0.41 | 0.34 |
| 20 | 0.22 | 0.60 | 0.12 | 0.58 | 0.16 | 0.17 | 0.24 | 0.23 | 0.55 | 0.17 | 0.99 | 0.13 | 0.01 | 0.38 | 0.10 | 0.45 |
| μ | 0.40 | 0.57 | 0.38 | 0.46 | 0.40 | 0.44 | 0.31 | 0.37 | 0.58 | 0.34 | 0.59 | 0.31 | 0.34 | 0.51 | 0.32 | 0.57 |
| σ | 0.19 | 0.25 | 0.25 | 0.28 | 0.23 | 0.21 | 0.23 | 0.21 | 0.27 | 0.20 | 0.33 | 0.25 | 0.20 | 0.28 | 0.26 | 0.27 |
| μ (ALL COLUMNS) = 0.43 | | | | | σ (ALL COLUMNS) = 0.26 | | | | | | | | | | | |

In this part of the paper the combination factor given in Eq. 1 ($\lambda$) required to equal the combined response given by the 30% rule to the exact response (reference response) obtained from the simultaneous application of both components, is estimated. The combination factor is defined as $\lambda_{req}$ in this case. Let us define $R_{exa}$ as the reference response and $R_{max}$ and $R_{min}$ as the maximum and the minimum of the individual effects. Then $\lambda_{req}$ can be obtained by

$$\lambda_{req} = \frac{R_{exact} - R_{max}}{R_{min}} \tag{5}$$

Since both rules reasonably overestimate the combined base shear, the $\lambda_{req}$ parameter is estimated only for axial loads. The values of $\lambda_{req}$ are presented in Table 11 for Model 2 and inelastic analysis. In the symbols $^iR_j$ used in the table, the left super-index $i$ represents the Load Cases 3, 4, 7 and 8, and the right sub-index $j$ stands for normal ($n$) and principal components ($p$). Hence, $^8R_p$ indicates the values of $\lambda_{req}$ correspond to Load Case 8 and principal components. Results of the table indicate that $\lambda_{req}$ significantly varies from one earthquake to another and from one column to another, as expected. Results for elastic analysis and Model 1are also estimated but are not shown, the mean values and standard deviations are quite similar to those presented in Table 11. It is observed from these results that, if the percentage rule is used, at least a value of 45% should be used for the combination factor in order to reduce the error in the estimation of the combined response.

## 5. Conclusions

When a structure is seismically analyzed, two horizontal recorded components are generally applied along their two major axes, sometimes ignoring the orientation of maximum response. In routine simplified analyses, structural responses are estimated by applying each component one at a time and then their effects are combined in many different ways. This concept has been implemented in many codes. The commonly used procedures are the 30 percent (30%) and the Square Root of Summation Squares (SRSS) combination rules. The basic assumption of these rules is that there is no correlation between the effects of the individual components. The accuracy of these rules and some related issues are addressed in this paper. They are: a) the critical orientation of the orthogonal components for collinear and non-collinear response quantities, b) the accuracy of the commonly used combination rules for complex MDOF systems for elastic and inelastic behavior and for collinear en non-collinear response parameters, and c) the accuracy of the rules for SDOF systems. To meet the objectives of the study, the seismic responses of some structural models used in the SAC steel project are estimated as accurately as possible. The particular case of steel buildings with moment resisting steel frames is considered. The study is also performed for equivalent SDOF systems.

Results of the study indicate that, for complex MDOF systems and earthquake loading, in general, the principal components give the maximum seismic response. For normal and principal components, both combination rules underestimate the axial load by about 10% and the COV of the underestimation is about 20%. Both rules overestimate the base shear by about 10%. The uncertainty in the estimation is much larger for axial load than for base shear. The mean axial loads and base shear values are essentially the same for elastic and inelastic behavior. However, the uncertainty in the prediction of axial load goes up significantly when inelastic behavior is considered. It is observed that the effect of individual components may be highly correlated, not only for normal components, but also for totally uncorrelated (principal) components, contradicting what stated in earlier investigations. Moreover, the rules are not always inaccurate in the estimation of the combined response for large values of correlation coefficients of the individual effects, and small values of such coefficients are not always related to an accurate estimation of the combined response.

For elastic SDOF systems and harmonic loading, depending on the column location, the 30% and SRSS rules may underestimate or overestimate the combined elastic axial load for totally correlated components. For perfectly uncorrelated components, the rules accurately estimate the elastic axial load. However, for inelastic behavior, the rules may underestimate or overestimate the combined axial load even for perfectly uncorrelated components. The combined base shear is reasonably overestimated practically in all the cases. For the case of SDOF systems and earthquake loading, both rules may underestimate or overestimate the combined response, however, on an average basis they reasonably estimate it for axial load and total base shear, for elastic an inelastic behavior.

Thus, only for the case of perfectly uncorrelated harmonic excitations and elastic analysis of SDOF systems, the individual effects of the components are uncorrelated and the 30% and SRSS rules accurately estimate the combined response. It is the authors' belief that the combination rules under consideration were developed for SDOF systems. In the general case, the level of underestimation or overestimation of the response depends on the level of correlation of the components, the type of structural systems, the type of response parameter, the location of the structural member under consideration and the level of structural deformation. The codes should be more specific regarding the applications of the mentioned commonly used combination rules. It is observed from the results that, if the percentage rule is used for MDOF systems and earthquake loading, at least a value of 45% should be used for the combination factor in order to reduce the error in the estimation of the combined response.

## Acknowledgements

This paper is based on work supported by El Consejo Nacional de Ciencia y Tecnología (CONACyT) under grant 50298-J and by La Universidad Autónoma de Sinaloa (UAS) under grant PROFAPI-2010/113. Any opinions, findings, conclusions, or recommendations expressed in this publication are those of the authors and do not necessarily reflect the views of the sponsors.

## References

Beyer, K. and Bommer J.J. (2007), "Selection and scaling of real accelerograms for bi-directional loading: a review of current practice and code provisions", *J. Earth. Eng.*, **11**(1), 13-45.

Bisadi, V. and Head, M. (2010), "Orthogonal effects in nonlinear analysis of bridges subjected to multi-component earthquake excitation", *Structures Congress of the American Society of Civil Engineers*, Section Bridges, 204-215.

Bojorquez, E., Reyes-Salazar A., Terán-Gilmore A. and Ruiz, S.E. (2010), "Energy-based damage index for steel structures", *Steel Compos. Struct, An International Journal*, **10**(4), 331-348.

Building Officials & Code Administration International (1993), 12th Edition, National Building Code.

Clough, R.W. and Penzien, J. (1993), *Dynamics of Structures*, Second Edition, McGraHill.

Gao, L. and Haldar, A. (1995) "Nonlinear seismic response of space structures with PR connections," *International Journal of Microcomputers in Civil Engineering*, **10**(1), 27-37.

Der Kiureghian, A. (1981), "A response spectrum method for random vibration analysis of MDOF systems, *Earth. Eng. Struct. D.*, **9**(5), 419-435.

Federal Emergency Management Agency (2000), State of the Art Report on Systems Performance of Steel Moment Frames Subjected to Earthquake Ground Shaking, SAC Steel Project, Report FEMA 355C.

Haldar, A. and Nee, K.M. (1989) "Elasto-plastic Large Deformation Analysis of PR Steel Frames for LRFD", *Compu. Struct.*, **31**(5), 811-823.

Hernández, J.J., López, O.A. (2003), "Evaluation of combination rules for peak response calculation in three-component seismic analysis", *Earth. Eng. Struct. D.*, **32**(10), 1585-1602.

International Code Council (2003), *International Building Code (IBC)*, Falls Church, VA.

Kondo, K. and Atluri, S.N. (1987), "Large deformation elasto-plastic analysis of frames under non-conservative loading using explicitly derived tangent stiffness based on assumed stress", *Comput. Mech.*, **2**(1), 1-25.

Kunnath, S.K., Erduran, E., Chai, Y.H. and Yashinsky, M. (2008), "Effect of near-fault vertical ground motions on seismic response of highway overcrossings," *J. Bridge Eng.*, **13**(3), 282-290.

Lopez, O.A., Chopra, A.K. and Hernandez, J.J. (2000) "Critical response of structures to multi-component earthquake excitation", *Earth. Eng. Struct. D.*, **29**, 1759-1778.

Lagaros (2010), "Multicomponent Incremental Dynamic Analysis considering variable incident angle", *J. Struct. Infrastructure Eng.*, **6**(2),77-94.

Lopez, O.A. and Torres, R. (1996), "A clarification of orthogonal Effects in a three- dimensional seismic analysis", *Earth. Spectra*, **12**, 357-361.

Lopez, O.A., Chopra, A.K and Hernandez, J.J. (2004), "Adapting the CQC3 rule for three seismic components

with different spectra", *J. Struct. Eng, ASCE*, **130**(3), 403-410.
Lopez, O.A., Chopra, A.K and Hernandez, J.J. (2001), "Evaluation of combination rules for maximum response calculation in multi-component seismic analysis", *Earth. Eng. Struct. D.*, **30**(9), 1379-1398.
Lopez, O.A, Hernandez J.J., Bonilla, R. and Fernandez A. (2006), "Response spectra for multi-component structural analysis, *Earth. Spectra*, **22**(1), 85-113.
Mackie, K.R. and Cronin K.J. (2011), "Response sensitivity of highways bridges to randomly oriented multi-component earthquake excitation", *J. Earth. Eng.*, **15**(6), 850-876.
McKenna, F. and Feneves, G.L. (2009). "Open system for earthquake engineering simulation." Pacific earthquake engineering research center, version 2.1.0.
Menun, C. and Der Kiureghian, A. (2000), "Envelopes for seismic response vectors. I: Theory", *J. Struct. Eng, ASCE*, **126**(4), 467-473.
Menun, C. and Der Kiureghian, A. (1998), "A replacement for the 30%, 40% and SRSS rules for multi-component seismic analysis", *Earth. Spectra*, **14**(1), 153-156.
Newmark, N.M. (1975) "Seismic design criteria for structures and facilities, Trans-Alaska pipeline system", *Proceedings of the U.S. National Conference on Earthquake Engineering,* pp. 94-103.
Newmark, N.M. and Hall, W.J. (1982), *Earthquake Spectra and Design*, Monograph Series, Earthquake Engineering Institute, Berkeley CA, USA.
Nielson, B. G. and DesRoches, R. (2006), "Influence of modeling assumptions on the seismic response of multi-span simply supported steel girder bridges in moderate seismic zones," *Eng. Struct.*, **28**(8), 1083-1092.
Penzien, J. and Watabe, M. (1975), "Characteristics of 3-dimensional earthquake ground motions," *Earthquake Engineering and Structural Dynamics*, **3**(4), 365-373.
Reglamento de construcciones del Distrito Federal (2004), Normas Técnicas Complementarias de Diseño por Sismo, *Gaceta Oficial del Distrito Federal*.
Reyes-Salazar, A., Haldar, A. and Romero-Lopez, M.R. (2000), "Force reduction factor for SDOF and MDOF", *Joint Specialty Conference on Probabilistic Mechanics and Structural,* ASCE, Paper 063.
Reyes-Salazar, A. (1997) " Inelastic Seismic Response and Ductility Evaluation of Steel Frames with Fully, Partially Restrained and Composite Connections," *PhD. thesis Department of Civil Engineering and Engineering Mechanics, University of Arizona,* Tucson, Arizona.
Reyes-Salazar, A. and Haldar, A. (1999), "Nonlinear seismic response of steel structures with semi-rigid and composite connections", *J. Constr. Steel Res.*, **51**, 37-59.
Reyes-Salazar, A. and Haldar, A. (2000), "Dissipation of energy in steel frames with pr connections", *Struct. Eng. Mech, An International Journal,* **9**(3), 241-256.
Reyes-Salazar, A. and Haldar, A. (2001a) "Energy dissipation at PR frames under seismic loading", *J. Struct. Eng*, *ASCE*, **127**(5), 588-593.
Reyes-Salazar, A. and Haldar, A. (2001b), "Seismic response and energy dissipation in partially restrained and fully restrained steel frames: An analytical study", *Steel*, *Compos. Struct., An International Journal,* **1**(4), 459-480.
Reyes-Salazar, A., Juarez-Duarte, J.A., López-Barraza, A. and Velázquez-Dimas, J.I. (2004), "Combined effect of the horizontal components of earthquakes for moment resisting steel frames", *Steel*, *Compos. Struct*, *An International Journal,* **4**(3), 89-209.
Reyes-Salazar, A., López-Barraza, A., López-López, L.A. and Haldar, A. (2008), "Multiple-components seismic response analysis–a critical review", *J. Earth. Eng.*, **12**(5), 779-799.
Rigato, A. B. and Medina, R. A. (2007), "Influence of angle of incidence on seismic demands for inelastic single-storey structures subjected to bi-directional ground motions," *Engineering Structures*, **29**(10), 2593-2601.
Rosenblueth, E. (1980), Design of Earthquake Resistance Structures, *Pentech Press* Ltd.
Rosenblueth, E. and Contreras, H. (1977), "Approximate design for multi-component earthquakes", *J. Eng. Mech. Division*, *ASCE*, **103**, 895-911.
Salmon, C.G., Johnson, J.E. and Malhas, F.A. (2009), *Steel Structures Design and Behavior*, 5th Edition, Pearson, Prentice Hall, New Jersey.
Smeby, W. and DerKiureghian, A. (1985), "Modal combination rules for multi-component earthquake excitation", *Earth. Eng. Struct. D.*, **13**(1), 1-12.
Shi, G. and Atluri, S.N. (1988), "Elasto-plastic large deformation analysis of spaces-frames", *Inter. J. Numer.*

*Meth. Eng.*, **26**, 589-615.
Uniform Building Code (1994), Structural Engineering Design Provisions Vol. 2, International Conference of Building Officials.
Wilson, E.L., Suharwardy, I. and Habibullah, A. (1995), "A clarification of the orthogonal effects in a three-dimensional seismic analysis", *Earth. Spectra,* **11**(4), 659-666.
Wilson, E.L., Der Kiureghian, A. and Bayo, E.P., (1981), "A replacement for the SRSS method in seismic analysis", *Earth. Eng. Struct. D.*, **9**(2), 187-194.

*CC*